Adaptive Global Sliding Mode Controller Design for Perturbed DC-DC Buck Converters

Saleh Mobayen [1,2,*,†] , Farhad Bayat [1,*,†] , Chun-Chi Lai [3] , Asghar Taheri [1] and Afef Fekih [4]

1   Department of Electrical Engineering, University of Zanjan, Zanjan 4537138791, Iran; taheri@znu.ac.ir
2   Future Technology Research Center, National Yunlin University of Science and Technology,
    Yunlin 64002, Taiwan
3   Bachelor Program in Interdisciplinary Studies, National Yunlin University of Science and Technology,
    Yunlin 64002, Taiwan; cclai@yuntech.edu.tw
4   Electrical and Computer Engineering Department, University of Louisiana at Lafayette,
    Lafayette, LA 70504, USA; afef.fekih@louisiana.edu
*   Correspondence: mobayen@znu.ac.ir (S.M.); bayat.farhad@znu.ac.ir (F.B.);
    Tel.: +98-24-33054219 (S.M.); +98-24-33054071 (F.B.)
†   These authors contributed equally to this work.

Abstract: This paper proposes a novel adaptive intelligent global sliding mode control for the tracking control of a DC-DC buck converter with time-varying uncertainties/disturbances. The proposed control law is formulated using a switching surface that eliminates the reaching phase and ensures the existence of the sliding action from the start. The control law is derived based on the Lyapunov stability theory. The effectiveness of the proposed approach is illustrated via high-fidelity simulations by means of Simscape simulation environment in MATLAB. Satisfactory tracking accuracy, efficient suppression of the chattering phenomenon in the control input, and high robustness against uncertainties/disturbances are among the attributes of the proposed control approach.

1. Introduction

DC-DC converters are widely employed in various electric power supply systems, such as DC motor drives, computers, cars, ships, aircraft, photovoltaic systems, etc. [1–4]. In those applications where the desired output voltage is smaller than the input voltage a common choice is the buck converter. Because of the nonlinear and time-varying structure of the buck converters owing to their switching operation, the design procedure of high-performance controller for these systems is a challenging topic [5–8]. The main objective of the control method is to confirm the stability of the system in the arbitrary condition with satisfactory dynamic response in the presence of load variations, parametric uncertainties and external disturbances. Nonlinear and robust control techniques are considered to be the best candidates in DC-DC converter applications than other linear feedback control methods. In the recent years, several nonlinear and robust control schemes have been employed for the stability and tracking control of DC-DC buck converters [9]. Among them, the sliding mode control (SMC) as an effective robust control method has received many applications because of its exceptional robustness against uncertainties and disturbances, guaranteed stability properties, computational and implementation easiness, fast response and excellent transient performance with respect to other control schemes [10,11]. The sliding mode control method has been prosperously applied to a broad diversity of practical linear and nonlinear systems such as nonholonomic systems [12,13], robot manipulators [14], aircraft [15], spacecraft [16,17], underwater vehicles [18], chaotic systems [19], electrical motors [20], and power systems [21,22]. The algorithm of SMC comprises two different phases, i.e., reaching and sliding phases [23]. Due to the impact of the switching

surface on the transient performance and stability of the closed-loop system, the main stage of SMC procedure is to present an appropriate sliding surface such that errors reduce to a suitable value [24,25]. In the traditional SMC design methods, the guaranteed performance of the robust tracking is only achieved after the states errors reach the sliding surface, and during the reaching phase the closed-loop system is not robust [26]. If the sliding action exists from the initial time, the system is more robust against perturbations compared to the conventional SMC with reaching phase. The global SMC (GSMC) method provides a unified framework to skip the reaching phase such that the sliding mode starts right from the beginning, and hence the controlled system is entirely invariant to the uncertainties and disturbances [27]. The global SMC yields a suitable robust performance when an additional term is inserted to the switching surface. In recent years, GSMC has become a noteworthy control procedure and its design algorithm is guaranteed to attain some particularly robust performance. In [28], an output-feedback GSMC scheme based on the high gain observer is presented for a class of SISO uncertain nonlinear systems. In [29], a novel discrete GSMC for DC-DC buck converters is introduced and the stability conditions for quasi-GSMC are proposed. In [30], a GSMC approach composed of optimal linear state-feedback and fuzzy nonlinear robust controllers is suggested for the electromechanical actuator of a missile with parametric external disturbances and variations. In [31], a global quasi-SMC (GQSMC) method is provided with guaranteed zigzag motion with a smaller bound compared to the method proposed by Gao. In [32], a GSMC disturbance-observer is proposed for the position tracking of DC motor system with parameter variations, modeling errors, and load moment disturbances. In [33], a chattering-free fuzzy back-stepping GSMC for tracking control of multi-joint robotic manipulators is proposed. In [34], a GSMC law based on linear matrix inequality (LMI) is designed for the stabilization of a class of nonlinear uncertain systems which guarantees the asymptotic stability of the states. In [35], an adaptive GSMC combined with an RBF neural network is suggested for the system identification, angular velocity estimation and tracking control of gyroscope system. In [36], an adaptive fast terminal SMC method combined with a GSMC scheme is proposed for the robust tracking control of uncertain third-order nonlinear systems. In [37], a solution to the design problem of adaptive GSMC based on dynamic nonlinear sliding function is proposed for linear helicopter systems with actuator faults and time-delays. To the best of our knowledge, no adaptive control method has been investigated to design a GSMC law for the tracking control of buck converters. This paper considers the tracking control problem of DC-DC buck converters with time-varying disturbances. To this aim, a robust controller is designed for the worst-case scenario and with the focus on the steady state response of the DC-DC buck converter (regulated DC value). The sliding mode control approach was used for its inherent robustness to input disturbances and the nature of its discontinuous control, which makes its implementation to power converters trivial [38]. Its main contributions are as follows:

- An adaptive GSMC approach based on the Lyapunov stability theorem to ensure the system is entirely invariant to the uncertainties and disturbances.
- A new switching surface that eliminates the reaching phase and ensures the existence of the sliding action from the start.
- A chattering-free robust control law that improve the robustness and stability of DC-DC buck converters.

It is emphasized that the transient behavior, intrinsic dynamics of the IGBT, and current and voltage fluctuations as a result of the inherent switching action of the buck converter were not the focus of this study. Nonetheless, the subject matter was the focus of various publications [39–41]. Moreover, most existing chips have mechanisms in place to counteract those ripples and over currents [42,43]. This paper is organized as follows. The dynamical model of DC-DC buck converter is briefly described in Section 2. The proposed adaptive global sliding mode controller is detailed in Section 3. The effectiveness of the proposed control scheme is illustrated in Section 4. Concluding remarks are finally given in Section 5.

2. Dynamical Model of DC-DC Buck Converter

The dynamical equations of the DC-DC buck converters for the switching situations ON and OFF are described as:

$$
\begin{aligned}
\dot{i}_L(t) &= \tfrac{1}{L}\left(v_{in}(t) - v_o(t)\right), \\
\dot{v}_o(t) &= \tfrac{1}{C}\left(i_L(t) - \tfrac{v_o(t)}{R}\right),
\end{aligned}
\tag{1}
$$

and

$$
\begin{aligned}
\dot{i}_L(t) &= -\tfrac{v_o(t)}{L}, \\
\dot{v}_o(t) &= \tfrac{1}{C}\left(i_L(t) - \tfrac{v_o(t)}{R}\right),
\end{aligned}
\tag{2}
$$

where R is the load resistor, C is the filter capacitor, L is the filter inductor, $v_{in}(t)$ denotes the DC input voltage, $i_L(t)$ represents the inductor current and $v_o(t)$ indicates the output voltage. Figure 1 displays the electrical circuit of the DC-DC buck converter.
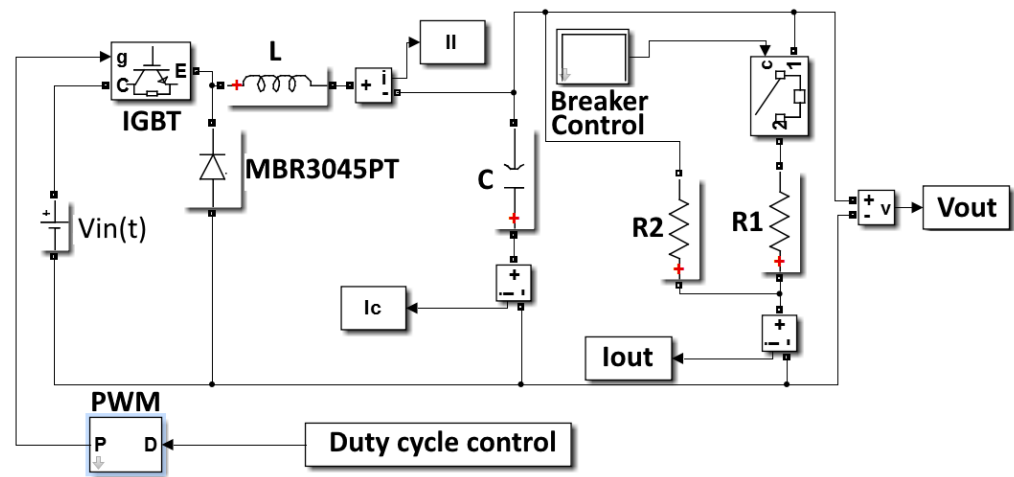

Figure 1. The DC-DC buck converter model in Simscape.

Considering (1) and (2), the dynamical model of DC-DC buck converter in both of the situations is given as:

$$
\begin{aligned}
\dot{i}_L(t) &= \tfrac{1}{L}\left(u(t)v_{in}(t) - v_o(t)\right), \\
\dot{v}_o &= \tfrac{1}{C}\left(i_L(t) - \tfrac{v_o(t)}{R}\right),
\end{aligned}
\tag{3}
$$

where u signifies the control input which takes 0 for OFF situation and 1 for ON situation of the switch (S_w). Now, considering the difference of the output voltage $v_0(t)$ and a continuous piecewise linear reference voltage $v_{ref}(t)$, we define the first state signal $e_1(t)$ as:

$$
e_1(t) = v_0(t) - v_{ref}(t).
\tag{4}
$$

Then, the second state variable is defined as:

$$
e_2(t) = \dot{e}_1(t) = \dot{v}_0(t) - \dot{v}_{ref}(t).
\tag{5}
$$

Then, considering that $\ddot{v}_{ref}(t) = 0$ (since $v_{ref}(t)$ is a continuous piecewise linear function), then dynamic model of the system's error in the state-space form can be expressed as:

$$
\begin{aligned}
\dot{e}_1(t) &= e_2(t), \\
\dot{e}_2(t) &= -\tfrac{e_2(t)}{RC} + \omega^2\left(u(t)v_{in}(t) - v_{ref}(t) - e_1(t)\right) + d(t),
\end{aligned}
\tag{6}
$$

where $\omega = \frac{1}{\sqrt{LC}}$ and $d(t)$ denotes an unknown disturbance signal with bounded amplitude, i.e., $|d(t)| \leq Q$. From practical point of view it is important to note that the values of resistors, capacitors and inductors used in the converter are not known exactly. This will

imply some uncertainties in the system's dynamic and should be considered in the design procedure to achieve more accurate and robust results. To this aim and assuming that the uncertainties are bounded we can represent the overall effects of those uncertainties by an uncertainty function $\psi(e_1, e_2, t)$ as:

$$
\begin{aligned}
\dot{e}_1(t) &= e_2(t), \\
\dot{e}_2(t) &= -\frac{e_2(t)}{R_0 C_0} + \omega_0^2 \Big(u(t) v_{in}(t) - v_{ref} - e_1(t) \Big) + \\
&\qquad \psi(e_1, e_2, t) + d(t),
\end{aligned}
\tag{7}
$$

where R_0, C_0 and L_0 are the nominal known values of the components, $\omega_0 = \frac{1}{\sqrt{L_0 C_0}}$ and it is assumed that the function $\psi(e_1, e_2, t)$ is unknown but bounded, i.e., $|\psi(e_1, e_2, t)| \leq \Psi$.

3. Main Results

In the DC-DC buck converters, the main goal is to regulate the output voltage at a desired value despite the existing disturbances/uncertainties. To this aim, we use the idea of global sliding mode control technique which is not only robust to perturbations such as the common sliding mode control approach, but also removes the reaching phase right from beginning. The following theorem characterizes the main results and provides the control law which guarantees the asymptotic convergence of the closed-loop system.

Theorem 1. *Consider the state-space model of DC-DC buck converter (3). If the control law is defined as follows, then the global asymptotic stability of the system is guaranteed and the output voltage regulation is achieved:*

$$
u(t) = -\frac{1}{v_{in} \omega_0^2} \left(
\begin{array}{l}
\frac{K}{g_\sigma} \operatorname{sgn}(e_2(t) + \phi e_1(0) e^{-\phi t}) - \frac{e_2(t)}{R_0 C_0} - \\
\omega_0^2 \Big(v_{ref} + e_1(t) \Big) - \phi^2 e_1(0) e^{-\phi t} + \\
\frac{g_s^2}{g_\sigma^2} \big(e_1(t) - e_1(0) e^{-\phi t} \big)
\end{array}
\right)
\tag{8}
$$

where ϕ, g_s and g_σ are the positive constants, and K is a positive coefficient with $K > g_\sigma(Q + \Psi)$.

Proof. Considering the output voltage regulation goal, the following sliding surfaces are defined:

$$
\begin{aligned}
s &= g_s \big(e_1(t) - e_1(0) e^{-\phi t} \big) \\
\sigma &= g_\sigma \big(e_2(t) + \phi e_1(0) e^{-\phi t} \big).
\end{aligned}
\tag{9}
$$

The time-derivative of the above sliding surfaces are written as

$$
\begin{aligned}
\dot{s} &= g_s \big(\dot{e}_1(t) + \phi e_1(0) e^{-\phi t} \big) \\
\dot{\sigma} &= g_\sigma \big(\dot{e}_2(t) - \phi^2 e_1(0) e^{-\phi t} \big).
\end{aligned}
\tag{10}
$$

Substituting (7) into (10), one achieves

$$
\begin{aligned}
\dot{s} &= g_s \big(e_2(t) + \phi e_1(0) e^{-\phi t} \big) \\
\dot{\sigma} &= g_\sigma \left(
\begin{array}{l}
\omega_0^2 \Big(u(t) v_{in}(t) - v_{ref} - e_1(t) \Big) - \frac{e_2(t)}{R_0 C_0} \\
+ \psi(e_1, e_2, t) + d(t) - \phi^2 e_1(0) e^{-\phi t}
\end{array}
\right).
\end{aligned}
\tag{11}
$$

Now, consider the following Lyapunov candidate function:

$$
V = \frac{1}{2}(s^2 + \sigma^2)
\tag{12}
$$

where differentiating V and using (11) yields

$$
\begin{aligned}
\dot{V} = {} & g_s\big(e_2(t) + \phi e_1(0)e^{-\phi t}\big)s \\
& + g_\sigma \left(\begin{array}{c} \omega_0^2\big(u(t)v_{in}(t) - v_{ref} - e_1(t)\big) - \frac{e_2(t)}{R_0 C_0} \\ + \psi(e_1, e_2, t) + d(t) - \phi^2 e_1(0)e^{-\phi t} \end{array} \right)\sigma
\end{aligned}
\tag{13}
$$

Substituting the suggested control law (8) into (13) and taking the definitions in (9) into account, one obtains

$$
\begin{aligned}
\dot{V} = {} & g_s \underbrace{\big(e_2(t) + \phi e_1(0)e^{-\phi t}\big)}_{\equiv \frac{\sigma}{g_\sigma}} s - K\mathrm{sgn}(\sigma)\sigma - \frac{g_s}{g_\sigma}s\sigma \\
& + g_\sigma \psi(e_1, e_2, t)\sigma + g_\sigma d(t)\sigma \\
= {} & \frac{g_s}{g_\sigma}\sigma s - K\mathrm{sgn}(\sigma)\sigma - \frac{g_s}{g_\sigma}s\sigma + g_\sigma \psi(e_1, e_2, t)\sigma \\
& + g_\sigma d(t)\sigma \\
= {} & \big(g_\sigma(\psi(e_1, e_2, t) + d(t)) - K\mathrm{sgn}(\sigma)\sigma\big) \\
\le {} & g_\sigma|\sigma|.|\psi(e_1, e_2, t) + d(t)| - K\underbrace{\mathrm{sgn}(\sigma)\sigma}_{|\sigma|} \\
\le {} & (g_\sigma(Q + \Psi) - K)|\sigma|
\end{aligned}
\tag{14}
$$

where considering the condition $K > g_\sigma(Q + \Psi)$ in (8), one obtains the asymptotic stability condition $\dot{V} < 0$. $\square$

Remark 1. *Compared to the common sliding surface $s_c = g_s e_1(t)$, the global sliding surface s in (9) forces the states of the system to arrive at the surface right from the beginning. Thus, the reaching mode is omitted, and the global robustness is fulfilled.*

In practice, the upper bounds of disturbances and uncertainties are often unknown and hence $|d(t)|$ and $|\psi(e_1, e_2, t)|$ are difficult to determine. Assume that disturbance and uncertainty terms are bounded, i.e., $Q > |d(t)|$, $\Psi > |\psi(e_1, e_2, t)|$, where Ψ and Q are two unknown positive constants. Moreover, assume that $\hat{Q}$ is the estimation of Q, $\hat{\Psi}$ is the estimation of Ψ, and $\hat{K}$ is the estimation of K with $\hat{K} > g_\sigma(\hat{Q} + \hat{\Psi})$ which is proposed by the subsequent adaptation law:

$$
\dot{\hat{K}} = \mu g_\sigma |\sigma|
\tag{15}
$$

where μ is a positive constant.

Theorem 2. *Consider the dynamical model of DC-DC buck converter (3). Let the sliding surface be in the form of (9) and suppose that the adaptation law (15) is satisfied. Using the adaptive control law specified by:*

$$
u(t) = -\frac{1}{v_{in}\omega_0^2} \left(\begin{array}{c} \frac{\hat{K}}{g_\sigma}\mathrm{sgn}(\sigma) - \frac{e_2(t)}{R_0 C_0} - \omega_0^2\big(v_{ref} + e_1(t)\big) \\ -\phi^2 e_1(0)e^{-\phi t} + \frac{g_s}{g_\sigma^2}s \end{array} \right)
\tag{16}
$$

then the global finite-time stability of the system is satisfied, and the output voltage regulation is achieved.

Proof. The positive-definite Lyapunov function candidate is considered to be:

$$
V = \frac{1}{2}(s^2 + \sigma^2) + \frac{1}{2}\chi \tilde{K}^2
\tag{17}
$$

where $\chi > 0$ and $\tilde{K} = \hat{K} - K$. Taking the time-derivative of V and using (15) and (16) gives

$$
\begin{aligned}
\dot{V} &= s\dot{s} + \sigma\dot{\sigma} + \chi\tilde{K}\dot{\hat{K}} \\
&= \frac{g_s}{g_\sigma}\sigma s + \chi\tilde{K}\dot{\hat{K}} - \frac{g_s}{g_\sigma}\sigma s + g_\sigma\psi(e_1, e_2, t)\sigma + \\
&\quad g_\sigma d(t)\sigma - \hat{K}|\sigma| \\
&= \chi\tilde{K}\mu g_\sigma|\sigma| + g_\sigma\psi(e_1, e_2, t)\sigma + g_\sigma d(t)\sigma - \hat{K}|\sigma|.
\end{aligned}
\tag{18}
$$

Equation (18) can be expressed as

$$
\begin{aligned}
\dot{V} &\le \mu g_\sigma\chi(\hat{K} - K)|\sigma| + g_\sigma|\psi(e_1, e_2, t)||\sigma| + \\
&\quad g_\sigma|d(t)||\sigma| - \hat{K}|\sigma| + K|\sigma| - K|\sigma| \\
&\le -(1 - \mu g_\sigma\chi)(\hat{K} - K)|\sigma| - \\
&\quad (K - g_\sigma|\psi(e_1, e_2, t)| - g_\sigma|d(t)|)|\sigma|.
\end{aligned}
\tag{19}
$$

Since $K > g_\sigma(|\psi(e_1, e_2, t)| + |d(t)|)$ and $\mu g_\sigma\chi < 1$, then Equation (19) can be represented as

$$
\begin{aligned}
\dot{V} &\le -(1 - \mu g_\sigma\chi)(\hat{K} - K)|\sigma| - g_\sigma(Q - |d(t)|)|\sigma| \\
&\quad -g_\sigma(\Psi - |\psi(e_1, e_2, t)|)|\sigma| \\
&\le -\sqrt{\frac{2}{\chi}}(1 - \mu g_\sigma\chi)|\sigma|\frac{(\hat{K} - K)}{\sqrt{\frac{2}{\chi}}} \\
&\quad -\sqrt{2}g_\sigma(Q - |d(t)|)\frac{|\sigma|}{\sqrt{2}} \\
&\quad -\sqrt{2}g_\sigma(\Psi - |\psi(e_1, e_2, t)|)\frac{|\sigma|}{\sqrt{2}} \\
&\le -\Xi\left(\frac{|s|}{\sqrt{2}} + \frac{|\sigma|}{\sqrt{2}} + \frac{\tilde{K}}{\sqrt{\frac{2}{\chi}}}\right) = -\Xi V^{\frac{1}{2}},
\end{aligned}
\tag{20}
$$

with $\Xi = \min\{\sqrt{2}g_\sigma(\Psi - |\psi(e_1, e_2, t)|), \sqrt{2}g_\sigma(Q - |d(t)|), \sqrt{\frac{2}{\chi}}(1 - \mu g_\sigma\chi)|\sigma|\} > 0$. Therefore, the adaptive global finite-time stability of the system is achieved, and the output voltage regulation is fulfilled. □

When the error trajectory is below the sliding surface, i.e., $S(e(t)) < 0$, the control signal must be applied ($u = 1$) such that it steers the error trajectory towards the sliding surface. In this situation (S_w : ON), to satisfy the reaching condition $S(e(t))\dot{S}(e(t)) < 0$, one obtains from (11) that:

$$
\begin{aligned}
&g_s\left(e_2(t) + \phi e_1(0)e^{-\phi t}\right) + \\
&g_\sigma\left(\begin{array}{l} -\frac{e_2(t)}{R_0 C_0} + \omega_0^2(v_{in}(t) - v_{ref} - e_1(t)) + \\ \psi(e_1, e_2, t) + d(t) + \phi e_2(0)e^{-\phi t} \end{array}\right) > 0.
\end{aligned}
\tag{21}
$$

On the other hand, when the error trajectory is above the sliding surface, i.e., $S(e(t)) > 0$, the control input must be disconnected ($u = 0$) such that it forces the error trajectory to move towards the sliding surface. In this situation (S_w : OFF), to fulfill the reaching condition, we achieve from (11) that:

$$
\begin{aligned}
&g_s\left(e_2(t) + \phi e_1(0)e^{-\phi t}\right) + \\
&g_\sigma\left(\begin{array}{l} -\frac{e_2(t)}{R_0 C_0} - \omega_0^2\left(e_1(t) + v_{ref}\right) + \\ \phi e_2(0)e^{-\phi t} + \psi(e_1, e_2, t) + d(t) \end{array}\right) < 0.
\end{aligned}
\tag{22}
$$

The overall control law which adapts such switching conditions is simplified as:

$$u(t) = \frac{1}{2}(1 - \text{sgn}(S(e(t))))$$
$$= \begin{cases} 1, & S(e(t)) < 0 \\ 0. & S(e(t)) > 0 \end{cases} \tag{23}$$

The direct realization of the controller (23) implies that the buck converter will operate at an infinite switching frequency which is not desirable in practice. Then, a hysteresis bandwidth *h* is employed for the control input:

$$u(t) = \begin{cases} 1, & S(e(t)) < -h \\ 0, & S(e(t)) > h \end{cases} \tag{24}$$

where if $S(e(t))$ is less than $-h$, the switch S_w will turn ON, and if $S(e(t))$ is more than h, the switch will turn OFF. The hysteresis modulation method limits the operating frequency of the switch. Considering the positive slope of the sliding surface by $\dot{S}(e(t))^+$ and the negative slope of it by $\dot{S}(e(t))^-$, the ON and OFF periods of the switch S_w are obtained as:

$$T_{ON} = \frac{2h}{\dot{S}(e(t))^+}, \tag{25}$$

$$T_{OFF} = \frac{-2h}{\dot{S}(e(t))^-}. \tag{26}$$

Now, assuming that the state errors $e_1(t)$ and $e_2(t)$ are negligible and the effect of the disturbance $d(t)$ and uncertainty $\psi(e_1, e_2, t)$ is removed, Equation (11) can be written as:

$$\dot{S}(e) \approx g_s \phi e_1(0)e^{-\phi t} + g_\sigma \left(\omega_0^2(u(t)v_{in} - v_{ref}) + \phi e_2(0)e^{-\phi t} \right), \tag{27}$$

where using (27), the ON and OFF periods (25) and (26) are calculated as:

$$T_{ON} = \frac{2h}{g_s \phi e_1(0)e^{-\phi t} + g_\sigma \left(\omega_0^2(v_{in} - v_{ref}) + \phi e_2(0)e^{-\phi t} \right)}, \tag{28}$$

$$T_{OFF} = \frac{-2h}{g_s \phi e_1(0)e^{-\phi t} + g_\sigma \left(-\omega_0^2 v_{ref} + \phi e_2(0)e^{-\phi t} \right)}. \tag{29}$$

Thus, the switching frequency can be achieved by:

$$f_s = \frac{1}{T_{ON} + T_{OFF}}$$
$$= \frac{\begin{pmatrix} \phi g_\sigma \omega_0^2 GE(0)e^{-\phi t}\left(2v_{ref} - v_{in}\right) + \\ g_\sigma^2 \omega_0^4 v_{ref}\left(v_{in} - v_{ref}\right) - \\ \phi^2 (GE(0))^2 e^{-2\phi t} \end{pmatrix}}{2g_\sigma h \omega_0^2 v_{in}}. \tag{30}$$

Considering $\lim_{t \to \infty} e^{-\phi t} = 0$ in the steady state, then (28) and (29) can be simplified as:

$$T_{ON} = \frac{2h}{g_\sigma \omega_0^2 (v_{in} - v_{ref})} \tag{31}$$

$$T_{OFF} = \frac{2h}{g_\sigma \omega_0^2 v_{ref}}. \tag{32}$$

Finally, using (31) and (32), the switching frequency is obtained by:

$$f_s = \frac{g_\sigma \omega_0^2 v_{ref}}{2h}\left(1 - \frac{v_{ref}}{v_{in}}\right), \tag{33}$$

This result signifies that the switching frequency is directly proportional to the sliding gain g_σ and inversely proportional to the hysteresis bandwidth h. These parameters can be chosen such that an appropriate switching frequency is obtained.

4. Simulation Results

In this section, the proposed GSMC design framework is implemented to control a DC-DC buck converter and its effectiveness and performance are verified. The verifications are performed using Simscape of the MATLAB software which is a high-fidelity simulation environment of the physical systems. The nominal parameters of DC-DC buck converter and its controller are presented in Table 1. In the following simulations, the total effects of the dynamic uncertainties and external disturbances are supposed as $\psi + d = 200\sin(2\pi t)$. These are additive disturbances that are modeled as entering the system in the same manner as the control input. They are implemented using an additional/summing block located at the input of the DC-DC block. It also assumed that the parameters of the converter have uncertainties with the magnitude of 10–20%, and the measurements of the DC-DC buck converter are contaminated with a Gaussian noise with zero mean, standard deviation of 0.1. First, the effects of load variation and the performance of the proposed controller to handle such situation is investigated. To this aim it is assumed that the output load is increased 100% at time 0.2 s, i.e., the output resistance changed from $R = 20\,\Omega$ to $R = 10\,\Omega$. The corresponding results of the converter output voltage $(v_o(t))$, the inductor current $(i_L(t))$ and the control signal $(u(t))$, are shown in Figure 2. The results demonstrate that the proposed method is able to stabilize very quickly the output voltage at the desired value $V_{ref} = 15$ volt, even for a large load variation. It is also observed from this figure that the inductor current varies from 0.75 to 1.5 ampere which itself determines the load current. Noticeably, the simulation results confirm the theoretical anticipations. In the second scenario, we investigate the performance of the proposed approach in the presence of load variations as well as disturbances and dynamic uncertainties, which will be introduced at time 0.4 s. The obtained results, in this case, are illustrated in Figure 3. The results demonstrate that the proposed method is able to robustly regulate the output voltage at the desired value $V_{ref} = 15$ volt in the presence of large load variation, uncertainties and disturbances. Finally, in the third scenario, it is assumed that the system is subject to the external disturbance of $d = 200\sin(2\pi t), \forall t >= 0.4$ s, the uncertainties in the converter's parameters (10–20%), and 100% output load variation (from 10 to 20 ohm). Then, assuming the desired output voltage $V_{ref} = 6$ volt, the simulation results are shown in Figure 4. It is seen that the proposed method is able to efficiently cope with all undesirable source of error affecting the system, i.e., load large variation, disturbances and parameter uncertainties.

Table 1. Parameters of DC-DC buck converter.

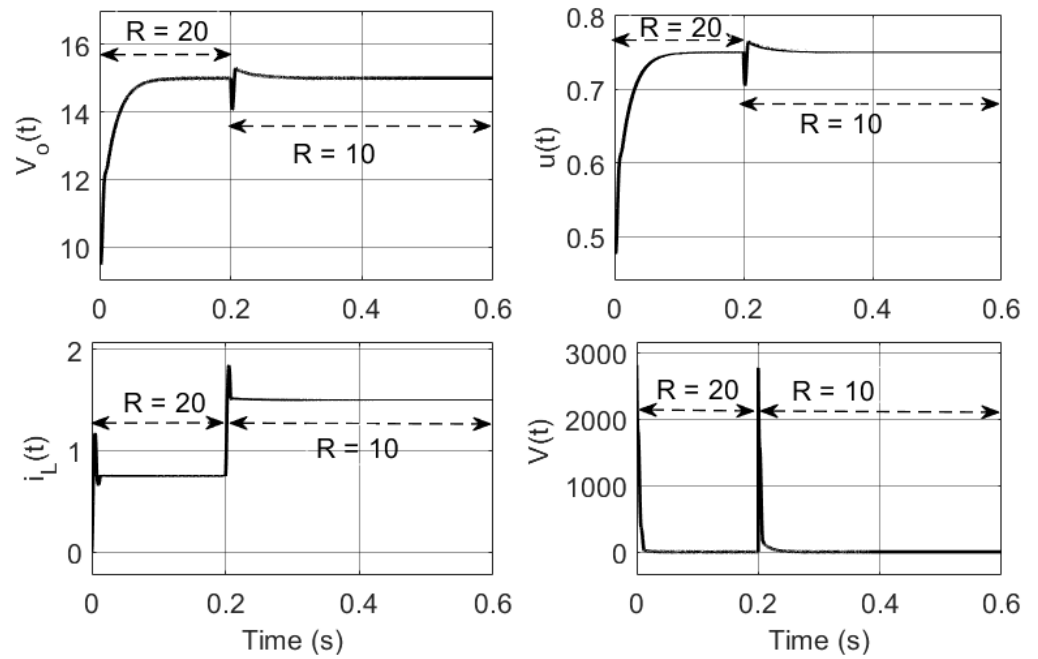| Param.	Value	Param.	Value	Param.	Value
C	1000 μF	g_s	60	χ	0.7
L	150 μH	g_σ	0.1	Q	3
R	20 Ω	ϕ	50	h	80
V_{in}	20 v	μ	0.5	K	10×10^3

Figure 2. Time trajectories of the output voltage $v_o(t)$, inductor current $i_L(t)$, control signal $u(t)$, and the Lyapunov function (Load variation).
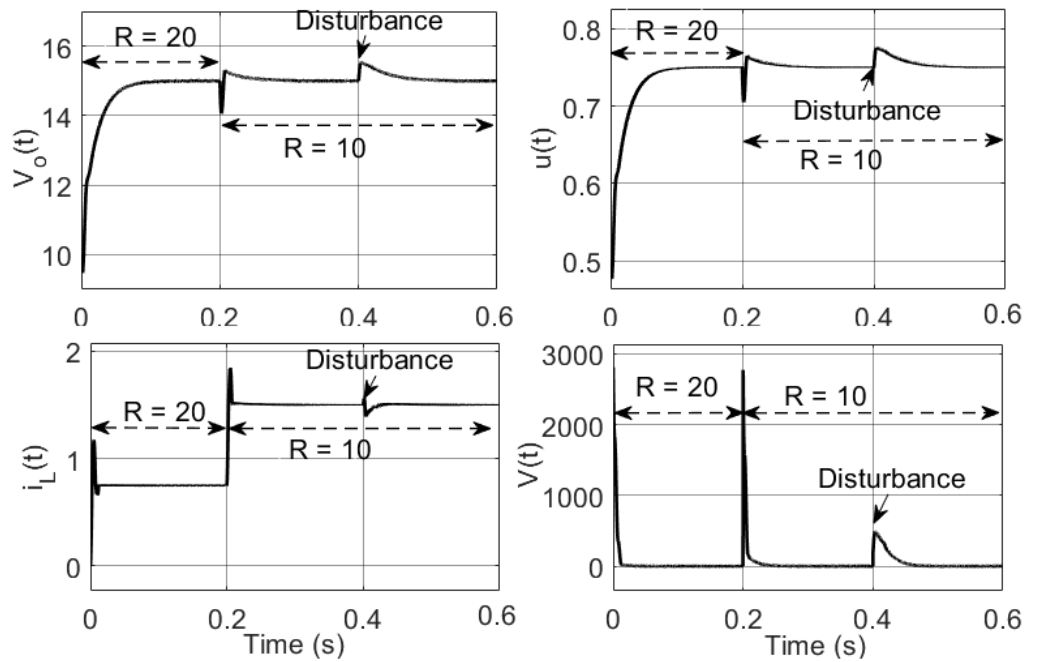

Figure 3. Time trajectories of the output voltage $v_o(t)$, inductor current $i_L(t)$, control signal $u(t)$, and the Lyapunov function (Load variation + disturbances).
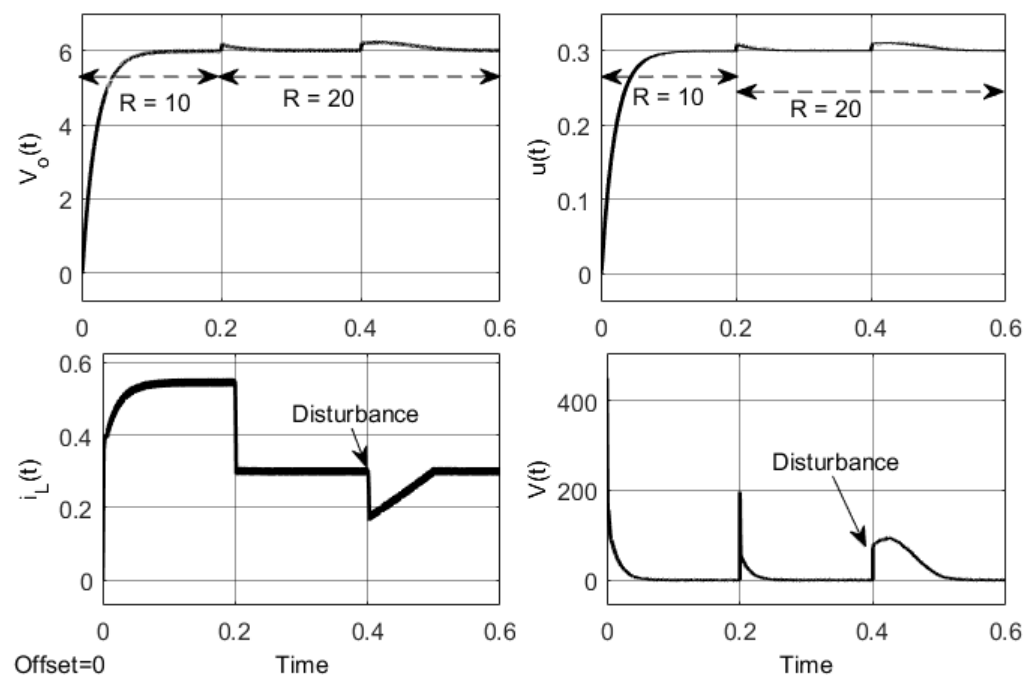
Figure 4. Time trajectories of the output voltage $v_o(t)$, inductor current $i_L(t)$, control signal $u(t)$, and the Lyapunov function (Load variation + disturbances + uncertainties).

5. Conclusions

This paper proposed a novel adaptive GSMC approach for DC-DC buck converters with time-varying uncertainties. The design was derived using a new switching surface and aimed at eliminating the reaching phase and ensuring system's global robustness and chattering-free dynamics. High-fidelity simulations conducted using Simscape simulation environment in MATLAB showed satisfactory tracking accuracy and high robustness against uncertainties/disturbances. Additionally, the design successfully suppressed the chattering phenomenon in the control input. It is worth noting that though in this paper we considered DC-DC buck converters, the proposed control framework is applicable to any high-order nonlinear system with bounded uncertainties.

References

1. Bayat, F.; Karimi, M.; Taheri, A. Robust output regulation of Zeta converter with load/input variations: LMI approach. *Control Eng. Pract.* **2019**, *84*, 102–111. [CrossRef]
2. Bensaada, M.; Stambouli, A.B. A practical design sliding mode controller for DC–DC converter based on control parameters optimization using assigned poles associate to genetic algorithm. *Int. J. Electr. Power Energy Syst.* **2013**, *53*, 761–773. [CrossRef]
3. Shtessel, Y.B.; Zinober, A.S.; Shkolnikov, I.A. Sliding mode control of boost and buck-boost power converters using method of stable system centre. *Automatica* **2003**, *39*, 1061–1067. [CrossRef]
4. Huangfu, Y.; Zhuo, S.; Rathore, A.K.; Breaz, E.; Nahid-Mobarakeh, B.; Gao, F. Super-twisting differentiator-based high order sliding mode voltage control design for DC-DC buck converters. *Energies* **2016**, *9*, 494. [CrossRef]

5.　Utkin, V. Sliding mode control of DC/DC converters. *J. Frankl. Inst.* **2013**, *350*, 2146–2165. [CrossRef]

6.　Deylamani, M.J.; Amiri, P.; Refan, M.H. Design and Stability Analysis of a Discrete-time Sliding Mode Control for a Synchronous DC-DC Buck Converter. *Int. J. Control Autom. Syst.* **2019**, *17*, 1393–1407. [CrossRef]

7.　Shtessel, Y.B.; Ghanes, M.; Ashok, R.S. Hydrogen Fuel Cell and Ultracapacitor Based Electric Power System Sliding Mode Control: Electric Vehicle Application. *Energies* **2020**, *13*, 2798. [CrossRef]

8.　Garriga-Castillo, J.A.; Valderrama-Blavi, H.; Barrado-Rodrigo, J.A.; Cid-Pastor, À. Analysis of Sliding-mode controlled impedance matching circuits for inductive harvesting devices. *Energies* **2019**, *12*, 3858. [CrossRef]

9.　Komurcugil, H. Non-singular terminal sliding-mode control of DC-DC buck converters. *Control Eng. Pract.* **2013**, *21*, 321–332. [CrossRef]

10.　Komurcugil, H. Adaptive terminal sliding-mode control strategy for DC-DC buck converters. *ISA Trans.* **2012**, *51*, 673–681. [CrossRef]

11.　Dev, A.; Sarkar, M.K. Robust higher order observer based non-linear super twisting load frequency control for multi area power systems via sliding mode. *Int. J. Control Autom. Syst.* **2019**, *17*, 1814–1825. [CrossRef]

12.　Chen, H.; Zhang, B.; Zhao, T.; Wang, T.; Li, K. Finite-time tracking control for extended nonholonomic chained-form systems with parametric uncertainty and external disturbance. *J. Vib. Control* **2018**, *24*, 100–109. [CrossRef]

13.　Narayan, S.; Kaur, S. Finite Time Fractional-Order Sliding Mode-Based Tracking for a Class of Fractional-Order Nonholonomic Chained System. *J. Comput. Nonlinear Dyn.* **2018**, *13*.

14.　Islam, S.; Liu, X.P. Robust sliding mode control for robot manipulators. *IEEE Trans. Ind. Electron.* **2010**, *58*, 2444–2453. [CrossRef]

15.　Alwi, H.; Edwards, C. Fault detection and fault-tolerant control of a civil aircraft using a sliding-mode-based scheme. *IEEE Trans. Control Syst. Technol.* **2008**, *16*, 499–510. [CrossRef]

16.　Bayat, F. Model predictive sliding control for finite-time three-axis spacecraft attitude tracking. *IEEE Trans. Ind. Electron.* **2018**, *66*, 7986–7996. [CrossRef]

17.　Bayat, F.; Javaheri, M. Two-Layer Terminal Sliding Mode Attitude Control of Satellites Equipped with Reaction Wheels. *Asian J. Control* **2020**, *22*, 388–397. [CrossRef]

18.　Zhu, D.; Sun, B. The bio-inspired model based hybrid sliding-mode tracking control for unmanned underwater vehicles. *Eng. Appl. Artif. Intell.* **2013**, *26*, 2260–2269. [CrossRef]

19.　Roohi, M.; Khooban, M.H.; Esfahani, Z.; Aghababa, M.P.; Dragicevic, T. A switching sliding mode control technique for chaos suppression of fractional-order complex systems. *Trans. Inst. Meas. Control* **2019**, *41*, 2932–2946. [CrossRef]

20.　Tota, A.; Lenzo, B.; Lu, Q.; Sorniotti, A.; Gruber, P.; Fallah, S.; Velardocchia, M.; Galvagno, E.; De Smet, J. On the experimental analysis of integral sliding modes for yaw rate and sideslip control of an electric vehicle with multiple motors. *Int. J. Automot. Technol.* **2018**, *19*, 811–823. [CrossRef]

21.　Ouassaid, M.; Maaroufi, M.; Cherkaoui, M. Observer-based nonlinear control of power system using sliding mode control strategy. *Electr. Power Syst. Res.* **2012**, *84*, 135–143. [CrossRef]

22.　Taherkhani, A.; Bayat, F. Wind turbines robust fault reconstruction using adaptive sliding mode observer. *IET Gener. Transm. Distrib.* **2019**, *13*, 3096–3104. [CrossRef]

23.　Zhao, Y.; Wang, J.; Yan, F.; Shen, Y. Adaptive sliding mode fault-tolerant control for type-2 fuzzy systems with distributed delays. *Inf. Sci.* **2019**, *473*, 227–238. [CrossRef]

24.　Liu, J.; Wu, L.; Wu, C.; Luo, W.; Franquelo, L.G. Event-triggering dissipative control of switched stochastic systems via sliding mode. *Automatica* **2019**, *103*, 261–273. [CrossRef]

25.　Sun, C.; Gong, G.; Yang, H. Sliding Mode Control with Adaptive Fuzzy Immune Feedback Reaching Law. *Int. J. Control Autom. Syst.* **2020**, *18*, 363–373. [CrossRef]

26.　Jiang, B.; Karimi, H.R.; Kao, Y.; Gao, C. A novel robust fuzzy integral sliding mode control for nonlinear semi-Markovian jump T-S fuzzy systems. *IEEE Trans. Fuzzy Syst.* **2018**, *26*, 3594–3604. [CrossRef]

27.　Xiu, C.; Guo, P. Global terminal sliding mode control with the quick reaching law and its application. *IEEE Access* **2018**, *6*, 49793–49800. [CrossRef]

28.　Peixoto, A.J.; Oliveira, T.R.; Hsu, L.; Lizarralde, F.; Costa, R.R. Global tracking sliding mode control for a class of nonlinear systems via variable gain observer. *Int. J. Robust Nonlinear Control* **2011**, *21*, 177–196. [CrossRef]

29.　Ni, Y.; Xu, J. Study of discrete global-sliding mode control for switching DC-DC converter. *J. Circuits, Syst. Comput.* **2011**, *20*, 1197–1209. [CrossRef]

30.　Liu, X.; Wu, Y.; Deng, Y.; Xiao, S. A global sliding mode controller for missile electromechanical actuator servo system. *Proc. Inst. Mech. Eng. Part J. Aerosp. Eng.* **2014**, *228*, 1095–1104. [CrossRef]

31.　Wu, M.; Chen, J.S. A discrete-time global quasi-sliding mode control scheme with bounded external disturbance rejection. *Asian J. Control* **2014**, *16*, 1839–1848. [CrossRef]

32.　Zhang, H.; Ge, L.; Shi, M.; Yang, Q. Research of compound control for DC motor system based on global sliding mode disturbance observer. *Math. Probl. Eng.* **2014**, *2014*, 1–7. [CrossRef]

33.　Shao, K.; Ma, Q. Global fuzzy sliding mode control for multi-joint robot manipulators based on backstepping. In *Foundations of Intelligent Systems*; Springer: Berlin/Heidelberg, Germany, 2014; pp. 995–1004.

34.　Mobayen, S. Design of LMI-based global sliding mode controller for uncertain nonlinear systems with application to Genesio's chaotic system. *Complexity* **2015**, *21*, 94–98. [CrossRef]

35. Chu, Y.; Fei, J. Adaptive global sliding mode control for MEMS gyroscope using RBF neural network. *Math. Probl. Eng.* **2015**, *2015*, 403180. [CrossRef]

36. Mobayen, S. An adaptive fast terminal sliding mode control combined with global sliding mode scheme for tracking control of uncertain nonlinear third-order systems. *Nonlinear Dyn.* **2015**, *82*, 599–610. [CrossRef]

37. Chen, F.; Jiang, R.; Wen, C.; Su, R. Self-repairing control of a helicopter with input time delay via adaptive global sliding mode control and quantum logic. *Inf. Sci.* **2015**, *316*, 123–131. [CrossRef]

38. Mehta, A.; Naik, B. *Sliding Mode Controllers for Power Electronic Converters*; Springer: Berlin/Heidelberg, Germany, 2019.

39. Amariutei, R.D.; Andries, V.D.; Goras, L.; Rafaila, M.; Buzo, A.; Pelz, G. On the transient analysis of a DC-DC buck converter under load steps scenarios. In Proceedings of the 2015 International Symposium on Signals, Circuits and Systems (ISSCS), Iasi, Romania, 9–10 July 2015; pp. 1–4

40. Hsu, Y.C.; Ting, C.Y.; Hsu, L.S.; Lin, J.Y.; Chen, C.C.P. A transient enhancement DC–DC buck converter with dual operating modes control technique. *IEEE Trans. Circuits Syst. II Express Briefs* **2018**, *66*, 1376–1380. [CrossRef]

41. Suntio, T. Methods to estimate load-transient response of buck converter under direct-duty-ratio and peak-current-mode control. *IEEE Trans. Power Electron.* **2019**, *35*, 6436–6446. [CrossRef]

42. Xie, H.; Guo, E. *How the Switching Frequency Affects the Performance of a Buck Converter*; Texas Instruments: Dallas, TX, USA, 2019.

43. Butterfield, B. Optimizing Transient Response of Internally Compensated dc-dc Converters with Feedforward Capacitor. Application Report; SLVA289; 2008. Available online: https://www.ti.com/lit/an/slva289b/slva289b.pdf?ts=1614329823364&ref_url=https%253A%252F%252Fwww.google.com%252F (accessed on 22 February 2021).